DOI: 10.1002/ejic.200500902

Iron(III) Complexes with the Ligand *N*′,*N*′-Bis[(2-pyridyl)-methyl]ethylenediamine (uns-penp) and Its Amide Derivative *N*-Acetyl-*N*′,*N*′-bis[(2-pyridyl)methyl]ethylenediamine (acetyl-uns-penp)

Jing-Yuan Xu,[a,b] Jörg Astner,[b] Olaf Walter,[c] Frank W. Heinemann,[d] Siegfried Schindler,*[b] Michael Merkel,[e] and Bernt Krebs*[e]

Keywords: Iron / Tripodal ligands / Catechol dioxygenase / Amide hydrogen bonding / Carboxamide coordination

Synthesis and structural characterization of the iron(III) complexes of the tripodal ligands *N*′,*N*′-bis[(2-pyridyl)methyl]-ethylenediamine (uns-penp), $[Fe(uns\text{-}penp)Cl_2]ClO_4 \cdot CH_3CN$, $[\{Fe(uns\text{-}penp)Cl\}_2O](ClO_4)_2 \cdot 2CH_3CN$ and the amide derivative *N*-Acetyl-*N*′,*N*′-bis[(2-pyridyl)methyl]ethylenediamine (acetyl-uns-penp), $[Fe_2(acetyl\text{-}uns\text{-}penp)_2O](ClO_4)_2 \cdot H_2O$, $[Fe(acetyl\text{-}uns\text{-}penp)(tcc)Br] \cdot (C_2H_5)_2O$ (tcc = tetrachlorocatecholate), and $[\{Fe(acetyl\text{-}uns\text{-}penp)(tcc)\}_2O] \cdot (C_2H_5)_2O \cdot CH_3OH$ are reported. Catechol dioxygenase reactivity of in situ prepared complex solutions was tested and showed that all complexes reacted slower compared with the iron tmpa system described in the literature.

Introduction

Tripodal ligands such as tris[(2-pyridyl)methyl]amine (tmpa, also abbreviated as tpa in the literature) as well as derivatives, e.g. N4Py (Scheme 1), have been used successfully in experimental studies to model copper and iron enzymes.[1–5] Iron(II) complexes of the related ligand Rtpen (R = Me, Bz etc.) were shown to react with an excess of hydrogen peroxide to form an end-on hydroperoxo complex that can convert to a side-on peroxo complex at higher pH values.[6–10] More recently it was demonstrated that iron complexes with the ligand Bztpen as well as N4Py can form an iron(IV) oxo species that is able to oxidise alkanes such as cyclohexane.[11]

Rtpen can be prepared in two different synthetic procedures. The first described previously starts from a monosubstituted ethylendiamine that is reacted with picolylchloride.[6–8] The second takes advantage of the amine *N*′,*N*′-bis[(2-pyridyl)methyl]ethylenediamine (uns-penp; Scheme 1), a versatile tripodal ligand described previously,[12,13] as a starting material. Interestingly, so far only an iron(II) complex of uns-penp has been described in the literature that has been investigated with regard to its spin crossover properties.[14] Furthermore, very recently an iron(II) complex of a derivative of uns-penp was described.[15] However, so far no iron(III) complexes have been described in the literature. Therefore, we decided to study the appropriate iron(III) complexes of this ligand as well as of its acetyl derivative *N*-acetyl-*N*′,*N*′-bis[(2-pyridyl)methyl]ethylenediamine (acetyl-uns-penp; Scheme 1), an amide that was obtained during the synthesis of uns-penp.

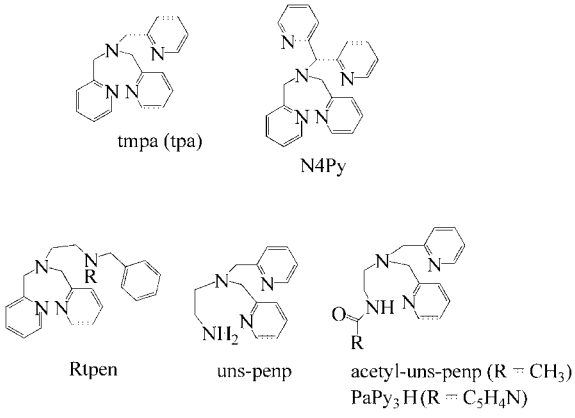

Scheme 1. The ligands discussed in the text.

Results and Discussion

Only recently have different research groups started to use uns-penp as a versatile ligand in different areas of coor-

[a] Pharmacy College, Tianjin Medical University, 300070 Tianjin, China
[b] Institut für Anorganische und Analytische Chemie der Justus-Liebig-Universität Gießen, Heinrich-Buff-Ring 58, 35392 Gießen, Germany
Fax: +49-641-9934149
E-mail: Siegfried.Schindler@chemie.uni-giessen.de
[c] Institut für Technische Chemie – Chemisch-Physikalische Verfahren (ITC-CPV), Forschungszentrum Karlsruhe, Postfach 3640, 76021 Karlsruhe, Germany
[d] Institut für Anorganische Chemie der Friedrich-Alexander-Universität Erlangen-Nürnberg, Egerlandstraße 1, 91058 Erlangen, Germany
[e] Institut für Anorganische und Analytische Chemie der Westfälischen Wilhelms-Universität, Wilhelm-Klemm-Straße 8, 48149 Münster, Germany
Fax: +49-251-83-38366
E-mail: krebs@uni-muenster.de

dination chemistry and different synthetic procedures have been described.[12,13,15–19] However, most of the authors unfortunately do not refer to the original synthesis of this ligand by Mandel and co-workers[12] and in one case it is presented a second time and described incorrectly as a new compound (ten years later in the same journal).[14] Some of us have used this ligand previously in studies within the field of copper chemistry and have improved its preparation.[13] During the two-step synthesis of uns-penp its protected form, *N*-Acetyl-*N*′,*N*′-bis[(2-pyridyl)methyl]ethylenediamine (acetyl-uns-penp), was easily obtained in pure form in high yields. Recrystallisation from petroleum ethers afforded single crystals that were suitable for X-ray diffraction studies. Acteyl-uns-penp crystallises with two molecules per unit cell. Those are dimerised by hydrogen bonding between the carboxamido group and one of the pyridine groups. The molecular structure of one of these dimers is presented in Figure 1 (see Table 2 for a summary of the crystallographic data and refinement parameters). Besides the hydrogen bonding, the crystal structure shows no extraordinary features.

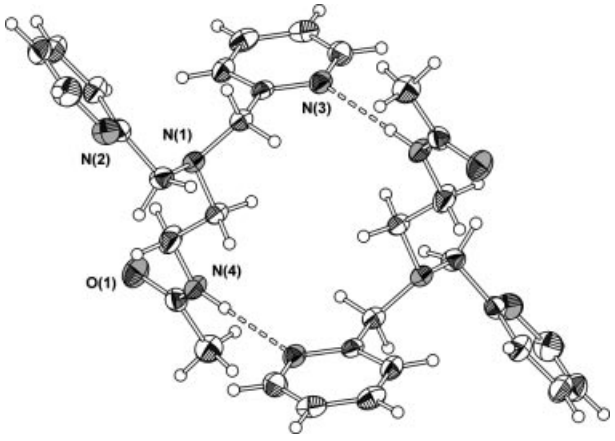

Figure 1. Thermal ellipsoid plot of an acetyl-uns-penp dimer (50% probability).

Furthermore, iron complexation with carboxamide ligands has attracted the interest of inorganic chemists to gain better understanding of metal–peptide bond coordination chemistry in life sciences[20] and to use such complexes as model compounds for the anti-tumor drug bleomycin[21,22] or nitrile hydratase.[23–25] Important in that regard are the results reported by Mascharak and co-workers, who have investigated in detail the structures and properties of Fe^{II}/Fe^{III} complexes of a number of carboxamide ligands, several based on a pyridine-2-carboxamide framework, e.g. *N*-{[bis(2-pyridylmethyl)amino]ethyl}pyridine-2-carboxamide ($PaPy_3H$).[22,25–31] The ligand $PaPy_3H$ (Scheme 1) is related to acetyl-uns-penp; instead of the methyl group in acetyl-uns-penp it contains an additional coordinating pyridyl unit.

$[Fe_2(acetyl\text{-}uns\text{-}penp)_2O](ClO_4)_2\cdot H_2O$ (1)

Acetyl-uns-penp has so far only been used to synthesise and characterise a copper(II) complex with this ligand. Herein the amide is not deprotonated, however, the carboxamido function of acetyl-uns-penp is no longer truly sp^2 hybridised and the nitrogen atom undergoes a weak interaction with the metal centre.[13] The copper complex of $PaPy_3H$ forms a dimer in which the oxygen atom of the amide is coordinated to the copper(II) ion.[32] In contrast, the iron amide complexes of $PaPy_3H$ described by Mascharak and co-workers contained the deprotonated ligand form.[27,30,32,33] However, our own efforts to synthesise the mononuclear deprotonated iron(III) complex [Fe(acetyl-uns-penp)]$(ClO_4)_2$ were only partially successful. Instead of the mononuclear species we obtained the dinuclear complex $[Fe_2(acetyl\text{-}uns\text{-}penp)_2O](ClO_4)_2\cdot H_2O$ (**1**). It is interesting to note at this point that the stoichiometrically identical compound $[Fe_2(PaPy_3H)_2O](ClO_4)_2$ (containing additional ethanol solvent molecules) derived through oxidation of the iron(II) complex is structurally completely different from **1**.[30] In this complex the oxo-bridge assembles two mononuclear amide complexes (with coordinated deprotonated amide nitrogen atoms while the oxygen atoms are not coordinated) to form the dimer (as one would expect). In contrast and as discussed below, in **1** the ligand acetyl-uns-penp additionally bridges the two iron(III) ions and involves the amide nitrogen as well as the oxygen atom in the coordination.

Crystals of **1** were at first obtained from the reaction of $Fe(ClO_4)_3$, acetyl-uns-penp and NaN_3 in methanol followed by recrystallisation of the precipitate in acetonitrile. In contrast to our expectations no azide complex was formed but instead deprotonation of the amide occurred under these conditions and because of the presence of water the oxo-bridged dinuclear complex **1** was obtained. Taking this result into account it was furthermore possible to crystallise **1** successfully by replacing the NaN_3 by Et_3N or NaOH as the deprotonating agent. The cation of **1**, as depicted in Figure 2, shows that the crystallographically equivalent iron(III) centres are triply bridged by one oxo and two carboxamido groups from two acetyl-uns-penp ligands, respectively, leading to an intramolecular Fe–Fe distance of 2.992 Å and an Fe–O–Fe angle of 113.1°. A summary of the crystallographic data and refinement parameters for the structures is presented in Table 2. Selected bond lengths and angles for the iron(III) complexes are reported in Table 1.

It is interesting to note that in **1**, the acetyl-uns-penp ligand shows an unusual pentadentate coordination mode displaying deprotonated carboxamido NCO bridging groups (η^2, μ_2) involving the delocalisation of π-bonding [*d*(C–O) = 1.283, *d*(C–N) = 1.306 Å], which is in agreement with the values of a related (η^2, μ_2) NCO-bridged iron complex reported previously.[34] However, in contrast, structural properties of **1** are quite different to a related iron(III) complex with a bridging urea anion.[35] Compared to other di-iron(III) complexes with three bridging ligands, of which at least one is a μ-oxo unit, **1** exhibits some unique structural features. The Fe–Fe separation is significantly shorter than those of other μ-oxo-tribridged diiron(III) complexes (range 3.048–3.335 Å) and the Fe–O–Fe angle is among the smallest of them all (range 113.8–134.7°).[36] Each iron(III) ion

Table 1. Selected distances [Å] and angles [°] in **1**–**5**.[a]

Atoms	**1**	Atoms	**2**	**3**	Atoms	**4**	Atoms	**5**
Fe(1)–O(1)	1.792(2)	Fe(1)–X	2.4813(9)	1.7929(5)	Fe(1)–N(1)	2.127(2)	Fe(1)–O(1)	1.798(1)
Fe(1)–O(2A)	2.013(2)	Fe(1)–O(2)	1.961(3)	2.012(2)	Fe(1)–N(3)	2.136(2)	Fe(1)–N(3)	2.141(2)
Fe(1)–N(4)	2.100(2)	Fe(1)–O(3)	1.969(3)	2.008(2)	Fe(1)–N(4)	2.172(2)	Fe(1)–N(1)	2.147(2)
Fe(1)–N(2)	2.157(2)	Fe(1)–N(1)	2.266(4)	2.366(3)	Fe(1)–N(2)	2.214(2)	Fe(1)–N(2)	2.213(2)
Fe(1)–N(3)	2.162(2)	Fe(1)–N(2)	2.191(4)	2.170(3)	Fe(1)–Cl(1)	2.2622(5)	Fe(1)–N(4)	2.235(2)
Fe(1)–N(1)	2.245(2)	Fe(1)–N(3)	2.159(4)	2.175(2)	Fe(1)–Cl(2)	2.3081(6)	Fe(1)–Cl(1)	2.3166(4)
O(1)–Fe(1A)	1.792(2)	Fe(1)···Fe(1A)		3.586			O(1)–Fe(1A)	1.798(1)
O(2)–Fe(1A)	2.013(2)	Fe(1)···N(4)		3.692(3)			Fe(1)···Fe(1A)	3.596(1)
Fe(1)···Fe(1A)	2.992(1)	O(2)···N(4)		2.755(3)				
O(1)–Fe(1)–O(2A)	98.35(5)	X–Fe(1)–O(2)	96.2(2)	98.25(6)	N(1)–Fe(1)–N(3)	153.61(6)	O(1)–Fe(1)–N(3)	93.26(3)
O(1)–Fe(1)–N(4)	103.62(6)	X–Fe(1)–O(3)	99.8(2)	106.26(7)	N(1)–Fe(1)–N(4)	83.51(6)	O(1)–Fe(1)–N(1)	90.95(3)
O(2A)–Fe(1)–N(4)	93.13(7)	X–Fe(1)–N(1)	165.6(2)	161.78(7)	N(3)–Fe(1)–N(4)	90.55(6)	N(3)–Fe(1)–N(1)	153.72(5)
O(1)–Fe(1)–N(2)	102.11(6)	X–Fe(1)–N(2)	93.5(2)	95.87(7)	N(1)–Fe(1)–N(2)	78.07(6)	O(1)–Fe(1)–N(2)	93.08(3)
O(2A)–Fe(1)–N(2)	85.80(6)	X–Fe(1)–N(3)	95.4(2)	92.24(7)	N(3)–Fe(1)–N(2)	75.55(6)	N(3)–Fe(1)–N(2)	76.04(4)
N(4)–Fe(1)–N(2)	154.12(7)	O(2)–Fe(1)–O(3)	82.9(2)	81.31(8)	N(4)–Fe(1)–N(2)	79.08(6)	N(1)–Fe(1)–N(2)	77.84(4)
O(1)–Fe(1)–N(3)	96.96(5)	O(2)–Fe(1)–N(1)	95.4(2)	95.28(9)	N(1)–Fe(1)–Cl(1)	105.57(4)	O(1)–Fe(1)–N(4)	170.11(3)
O(2A)–Fe(1)–N(3)	164.53(6)	O(2)–Fe(1)–N(2)	168.1(2)	160.74(9)	N(3)–Fe(1)–Cl(1)	100.04(4)	N(3)–Fe(1)–N(4)	88.86(4)
N(4)–Fe(1)–N(3)	85.43(7)	O(2)–Fe(1)–N(3)	86.5(2)	96.38(9)	N(4)–Fe(1)–Cl(1)	89.42(4)	N(1)–Fe(1)–N(4)	82.98(4)
N(2)–Fe(1)–N(3)	88.81(6)	O(3)–Fe(1)–N(1)	90.1(2)	87.77(9)	N(2)–Fe(1)–Cl(1)	167.56(5)	N(2)–Fe(1)–N(4)	78.04(4)
O(1)–Fe(1)–N(1)	173.14(7)	O(3)–Fe(1)–N(2)	88.7(2)	82.20(9)	N(1)–Fe(1)–Cl(2)	89.33(5)	O(1)–Fe(1)–Cl(1)	102.82(2)
O(2A)–Fe(1)–N(1)	87.39(7)	O(3)–Fe(1)–N(3)	162.3(2)	161.50(9)	N(3)–Fe(1)–Cl(2)	92.30(5)	N(3)–Fe(1)–Cl(1)	100.45(3)
N(4)–Fe(1)–N(1)	79.68(7)	N(1)–Fe(1)–N(2)	76.2(2)	74.16(9)	N(4)–Fe(1)–Cl(2)	169.15(4)	N(1)–Fe(1)–Cl(1)	103.87(3)
N(2)–Fe(1)–N(1)	74.44(7)	N(1)–Fe(1)–N(3)	76.8(2)	74.12(9)	N(2)–Fe(1)–Cl(2)	91.49(4)	N(2)–Fe(1)–Cl(1)	163.93(3)
N(3)–Fe(1)–N(1)	77.19(7)	N(2)–Fe(1)–N(3)	99.5(2)	96.10(9)	Cl(1)–Fe(1)–Cl(2)	100.38(2)	N(4)–Fe(1)–Cl(1)	86.26(3)
Fe(1A)–O(1)–Fe(1)	113.1(2)	Fe(1A)–O(1)–Fe(1)		180			Fe(1A)–O(1)–Fe(1)	180

[a] X = Br(1) in **2** or O(4) in **3** A: *x*, *y*, –*z* + 1/2 (for **1**); –*x*, –*y*, –*z* (for **5**).

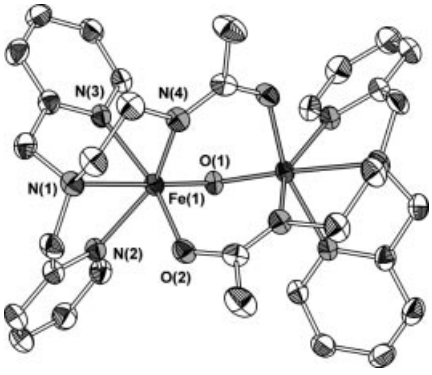

Figure 2. Thermal ellipsoid plot of the dinuclear complex in **1** (50% probability; hydrogen atoms omitted for clarity).

adopts a distorted octahedron coordination geometry by a N_4O_2 donor set, in which two pyridine nitrogen atoms (N2 and N3), one carboxamido nitrogen atom (N4) and a carboxamide oxygen atom (O2A) from the second acetyl-uns-penp ligand reside in the equatorial plane while oxo-bridged O(1) and the tertiary amino N(1) atoms occupy the axial positions. The negative charge of the μ-oxo-bridge leads to a rather short Fe(1)–O(1) bond [1.792(2) Å] and likewise because of the *trans* effect, the opposing Fe(1)–N(1) bond is weakened with a distance of 2.245(2) Å. All *cis* angles around O(1) are larger than the ideal 90°, with values of 98.35(5)° for O(1)–Fe(1)–O(2A), 102.11(6)° for O(1)–Fe(1)–N(2), 96.96(5)° for O(1)–Fe(1)–N(3) and 103.62(6)° for O(1)–Fe(1)–N(4). Obviously, deprotonation of the carboxamide groups facilitates the increase of bond lengths around the Fe^{III} ions (Table 1).

Model Complexes for Intradiol Catechol Dioxygenases

One reason for our efforts to obtain the mononuclear iron(III) complex with the deprotonated acetyl-uns-penp as ligand was our hope that this complex might be an excellent functional model for intradiol catechol dioxygenases. These mononuclear nonheme iron enzymes catalyse the oxidative cleavage of catechol derivatives by insertion of both atoms of dioxygen into the substrate—a key step in the degradation of aromatic compounds.[4,37,38]

Since Funabiki et al. reported the first functional models for catechol dioxygenases, increased efforts have been made by bioinorganic chemists to mimic the structure and function of these enzymes.[4,37–42] Besides macrocyclic ligands,[43–45] especially tetradentate tripodal ligands have shown considerable abilities to regulate the properties of model complexes, indicating that dioxygenase activity strongly depends on the nature of the ligand. The most effective biomimetic catalyst to date is the iron(III) tmpa (tpa) complex that was first reported by Que and co-workers.[4,46] Furthermore, several other systems with tripodal N_4 donor ligands showed considerable catechol dioxygenase activity.[47,48] Complexes with enzyme-analogous N_2O_2 donor sets represent good structural and spectroscopic model compounds, however, they are poor functional models so far.[49–56] Our recent efforts to reach higher activities than

the iron(III) tmpa complex by increasing or decreasing the chelate ring sizes in this system were unsuccessful.[57]

The substrate-binding process in the reaction cycle of the catechol cleavage involves protonation of two ligands at the active site, Tyr447 and a hydroxide.[58,59] These two proton acceptors dissociate from the metal ion and thereby enable the proton donor molecule, the catechol, to coordinate in its dianionic form (see Scheme 2).

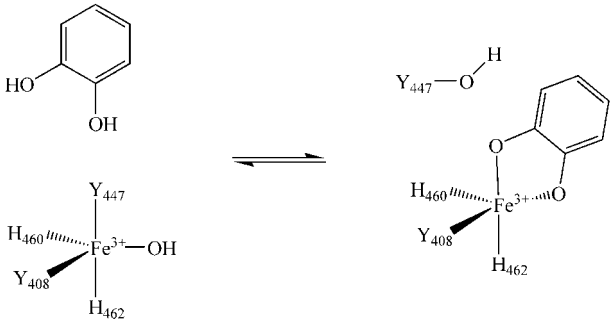

Scheme 2. Proposed substrate-binding process in catechol-1,2-dioxygenases.

The special electronic properties of the leaving Tyr447 group have been studied extensively using spectroscopic methods and seem to influence the reactivity of the enzyme to a large extent.[60] In previous work some of us used a tmpa-derived ligand [(6-bromo-2-pyridyl)methyl]bis[(2-pyridyl)methyl]amine (brtpa) to mimic the weak bonding of one of the donor groups, however, again it was observed that catechol dioxygenase reactivity decreased compared to the iron tmpa system, most likely because of steric hindrance.[61]

Replacing one pyridyl moiety of the tmpa ligand with a deprotonated carboxamide function we had hoped to finally increase reaction rates of the oxidation of catecholates compared to the tmpa system. However, as discussed below we did not reach this goal and furthermore, in contrast to the synthesis of complex **1**, we did not succeed in the preparation of deprotonated amide complexes when using acetyl-uns-penp, catecholates and base.

[Fe(acetyl-uns-penp)(tcc)Br]·$(C_2H_5)_2O$ (2)

When iron(III) bromide, acetyl-uns-penp, tetrachlorocatechol and triethylamine were mixed in acetone the complex [Fe(acetyl-uns-penp)(tcc)Br]·$(C_2H_5)_2O$ (**2**) was obtained. Slow diffusion of diethyl ether into the complex solutions allowed the precipitation of single crystals that were suitable for X-ray diffraction studies. Four complex molecules and four diethyl ether molecules form the unit cell of compound **2**. The diethyl ether molecules are attached to the complex via hydrogen bonding to the noncoordinating carboxamide function of the ligand. The structure of **2** is depicted in Figure 3 (the solvate molecule has been omitted for clarity; crystallographic data are presented in Table 2 and Table 1).

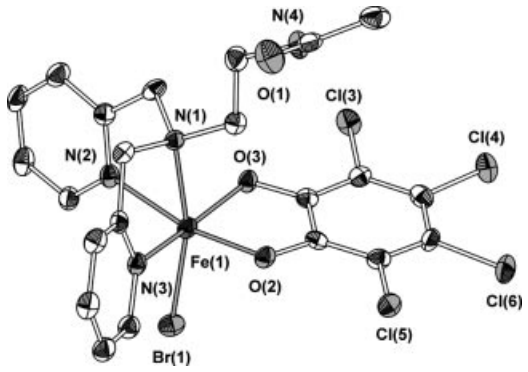

Figure 3. Thermal ellipsoid plot of the iron(III) complex in **2** (50% probability; hydrogen atoms omitted for clarity).

The iron(III) core is ligated by three nitrogen atoms, two catecholate oxygen atoms and one bromide atom. The longest bonds formed by iron and its donor atoms are found for Fe(1)–Br(1) and Fe(1)–N(1) with 2.4813(9) and 2.266(4) Å, respectively. This causes stretching of the coordination octahedron along the Br(1)–Fe(1)–N(1) axis. The *cis* angles around the bromide ion are widened to an average angle of 96.2°. On the other hand, the formation of five-membered chelate rings leads to small values for the N(1)–Fe(1)–N(2) and N(1)–Fe(1)–N(3) angles of 76.2(2) and 76.8(2)°, respectively.

[{Fe(acetyl-uns-penp)(tcc)}$_2$O]·$(C_2H_5)_2O$·CH_3OH (3)

Interestingly, applying the same experimental conditions as for the synthesis of **2**, though using a slightly larger amount of base, the dinuclear oxo-bridged complex [{Fe(acetyl-uns-penp)(tcc)}$_2$O]·$(C_2H_5)_2O$·CH_3OH (**3**) was obtained (the syntheses of **2** and **3** could be reproduced applying these conditions). The molecular structure of the cation of **3** is shown in Figure 4 (crystallographic data are presented in Table 2 and Table 1).

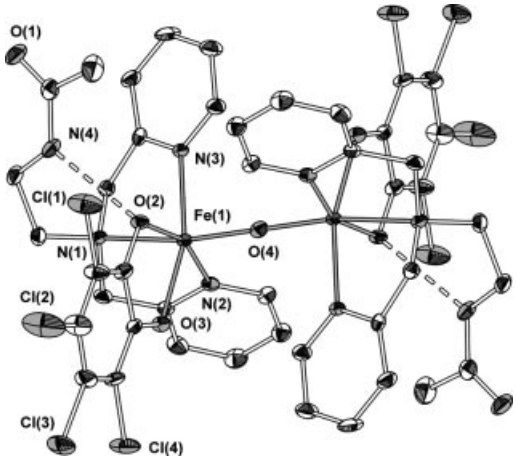

Figure 4. Thermal ellipsoid plot of the dinuclear complex in **3** (50% probability; hydrogen atoms omitted for clarity).

The unit cell contains two complexes as well as four diethyl ether and two disordered methanol molecules. Since

the bridging oxygen atom O(4) is located on a symmetry centre, one half of the dinuclear complex is generated by inversion. The metal–metal distance is 3.586 Å and both iron ions are surrounded by an N_3O_3 donor set. The nitrogen donor atoms are provided by the ligand acetyl-uns-penp, whereas the oxygen atoms belong to the dianionic tetrachlorocatecholate ligand and the μ-oxo-bridge. The coordination sphere of the iron centre has a distorted octahedral geometry. The negative charge of the μ-oxo-bridge leads to a rather short Fe(1)–O(4) bond (1.793 Å) and because of a *trans* effect, the opposing Fe(1)–N(1) bond is weakened. All *cis* angles around O(4) are larger than the ideal 90°. Especially those to the catecholate oxygen atoms are widened, since this effect can be attributed to electrostatic repulsion. The negative charge of O(2) is reduced by the intramolecular hydrogen bond and therefore the corresponding O(2)–Fe(1)–O(4) angle has a value of only 98.25(6)° compared to 106.29(9)° for O(3)–Fe(1)–O(4).

The most striking feature of **3** is the intramolecular hydrogen bond between the carboxamide nitrogen N(4) and O(2) of the catecholate. The donor acceptor distance has a typical value of 2.755(3) Å and the distance between Fe(1) and N(4) is 3.692 Å. This is in good agreement with similar intramolecular hydrogen bonding reported recently.[61] In a way this hydrogen bonding indicates a possible pathway for the deprotonation of the catechol similar to the enzyme reaction shown in Scheme 1.

Spectrophotometric Titrations

To gain a better understanding of the influence of the base and furthermore to achieve optimised conditions for catechol cleavage by molecular dioxygen it is necessary to provide a high concentration of the mononuclear iron complex with one coordinated catecholate dianion ([Fe(L)(3,5-dbc)]$^+$). To determine these ideal conditions for the catechol cleavage experiments, spectrophotometric titrations were performed (see Figure 5 and Exp. Sect.) as described previously for related systems.[61]

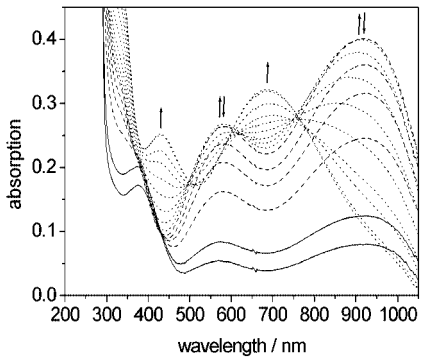

Figure 5. Spectrophotometric titration of a solution of iron(III) perchlorate hydrate, acetyl-uns-penp and 3,5-dbc against piperidine; solid lines: 0.0 and 0.5 equiv.; dashed lines: 1.0–1.6 equiv.; dotted lines: 1.8–4.0 equiv..

This analysis allowed us to gain insight into the species distribution in solution depending on the amount of external base that was added to a mixture of iron salt, the ligand and the substrate 3,5-dbc. At the beginning of the titration (0.0–0.5 equiv. of piperidine; piperidine was used for comparison with previous studies, however triethylamine works in the same way) an absorption band at 375 nm can be observed that is assigned to an oxo-iron(III)-CT transition.

We suggest that the main species in solution is a μ-oxo-bridged dinuclear compound without coordinated substrate. Such dinuclear complexes are thermodynamically favoured in the presence of water and many examples have been reported in the literature.[62–72] With regard to previous results it is possible that the carboxamido group of the ligand already undergoes a very weak interaction with the metal centre and is not truly sp^2 hybridised, however is not yet deprotonated.[13] Furthermore, two weak transitions occur at 580 and 920 nm which are typical for catecholate-iron(III)-CT transitions and indicate the presence of a low concentration of the desired mononuclear substrate adduct. Upon further addition of base (1.0–1.6 equiv.) these two absorption bands rise dramatically and so does the concentration of the mononuclear substrate adduct. In the last part of the titration (1.8–4.0 equiv.) the bands at 580 and 920 nm disappear and two new bands are seen at 430 and 690 nm that are also assigned to catecholate-iron(III)-CT transitions. The shift to higher energies indicates a higher electron density on the iron(III) core that makes the charge transfer from the catecholate more difficult. In accordance to the crystal structure of **3** we suggest that a dinuclear μ-oxo-bridged substrate adduct is formed in which the large electron density of the oxo-group is partially transferred to the metal ions and one ligand arm is detached. Finally, the amount of base that is necessary to reach optimal reaction conditions for the catechol cleavage was determined from a plot of the absorption of the lower energy CT band vs. the amount of base added (see Figure 6). The maximum of this plot is located at 1.7 equiv..

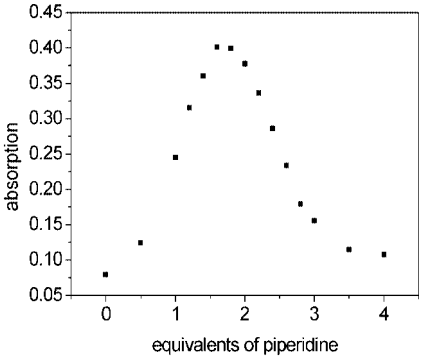

Figure 6. Absorbance vs. base equivalents plot (λ = 980 nm).

Catechol 1,2-Dioxygenase Activity

An in situ prepared complex solution containing equimolar amounts of iron(III) perchlorate hydrate and acetyl-uns-penp was treated with 1 equiv. of 3,5-dbc and 1.7 equiv. of piperidine. The decrease in the lower energy LMCT band

was monitored by UV/Vis-spectroscopy. The reaction was performed in air-saturated methanol, resulting in a more than tenfold excess of dioxygen that ensures pseudo-first-order kinetics for the complete reaction. From the slope of the ln(absorbance) vs. time plot, the reaction rate was determined to be 0.05 $M^{-1}s^{-1}$, which is more than two orders of magnitude lower than that reported for the iron-tmpa system under similar reaction conditions.[46] Because of this low reactivity no further experiments were performed with this system.

[Fe(uns-penp)Cl_2]ClO_4·CH_3CN (4)

The ligand uns-penp was obtained in good yields according to the procedures described in the literature. Mixing uns-penp together with iron(III) salts in methanol afforded a yellow material that could be recrystallised from acetonitrile by ether diffusion to yield crystals suitable for X-ray structural analysis. The ORTEP representation of [Fe(uns-penp)Cl_2]$^+$ is shown in Figure 7.

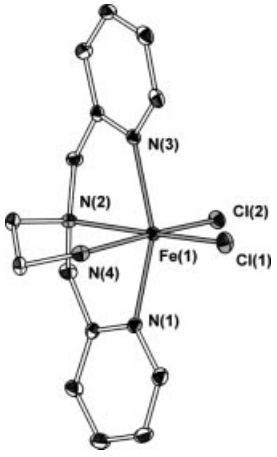

Figure 7. Thermal ellipsoid plot of the cation of **4** (50% probability; hydrogen atoms omitted for clarity).

The structure of the cation of **4** shows a distorted octahedral geometry coordinated with four N atoms of the uns-penp ligand and two chloride ions, as represented by the *trans* ligand angles of 153.61(6)° for N(1)–Fe(1)–N(3), 167.56(5)° for N(2)–Fe(1)–Cl(1), and 169.15(4)° for N(4)–Fe(1)–Cl(2). Moreover, the angle for Cl(1)–Fe(1)–Cl(2) is 100.38(2)°, which is significantly larger than 90°. As is often the case with a tripodal ligand that forms five-membered chelate rings, the coordination geometry is distorted toward the tertiary amino group (average N_{amine}–Fe–$N_{py/amine}$ = 77.55°). The Fe–N_{py} bonds (av. 2.132 Å) are shorter than the Fe–N(amine) bond (av. 2.193 Å), which are comparable to the values of Fe^{III} tmpa complexes.[46,73,74] Consequently the Fe(1)–Cl(1) bond which is *trans* to the tertiary amino group [2.2622(5) Å] is shorter than the Fe(1)–Cl(2) bond *trans* to a primary amino nitrogen [2.3081(6) Å].

{[Fe(uns-penp)Cl]$_2$O}$(ClO_4)_2$·$2CH_3CN$ (5)

It is well known that a general problem in iron(III) chemistry is the formation of oxo-bridged dimers during the synthesis of the complexes such as for example the iron(III) tmpa complex or the acetyl-uns-penp ligand system described above. Addition of base can accelerate this reaction and therefore when base was added during the synthesis of **4** the dinuclear oxo-bridged complex **5** was obtained instead. The thermal ellipsoid representation of the cation of **5** is shown in Figure 8. The molecular structure is composed of centrosymmetric dimeric cations with a linear Fe–O–Fe unit. Each iron centre is in a distorted octahedral environment ligated by the two pyridine nitrogen atoms, the primary and tertiary amine nitrogen atoms, as well as the oxygen atom which is bound to the second iron centre. The Fe–O bond length of 1.798(1) Å is in keeping with the mean values of 1.79(6) (with a range of 1.73–1.82 Å) for such bond lengths in oxo-bridged iron(III) complexes.[75] The Fe–N_{py} bonds of 2.141(2) Å and 2.147(2) Å are considerably shorter than the Fe–N_{amine} bonds [2.213(2) and 2.235(2) Å]. This is analogous to the structures of the respective (μ-oxo) diiron(III) complexes of tmpa. The chloride ligands coordinate *trans* to the tertiary amine nitrogen on each iron centre and *anti* to each other relative to the Fe–O–Fe axis. The Fe–Cl bond lengths of 2.3166(4) Å are slightly longer than the values of **4** arising from steric hindrance in the dimer. The Fe–Fe distance of 3.596 Å is typical for complexes with singly bridged Fe–O–Fe cores, which are usually in the range 3.4–3.6 Å, whereby the longer distances are associated with Fe–O–Fe angles that are linear or close to linearity.

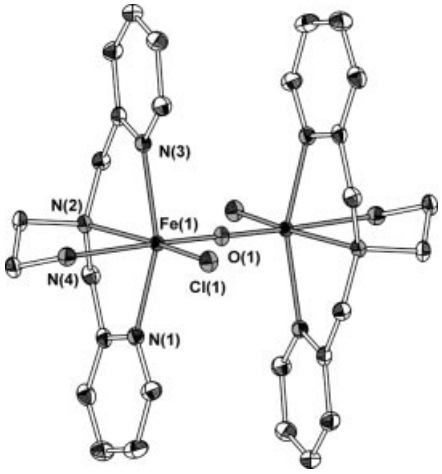

Figure 8. Thermal ellipsoid plot of the cation of **5** (50% probability; hydrogen atoms omitted for clarity).

Catechol 1,2-Dioxygenase Activity of the Iron(III)-uns-penp System

The iron(III)-uns-penp complex was investigated under the same conditions used previously for the iron(III) tmpa catecholate (3,5-dbc) system.[57] Stopped-flow kinetic investigations revealed again that the rate of the reaction of the iron tmpa system is faster under these conditions, however, at least the iron-uns-penp complex was only slower by a factor of 20. No further detailed kinetic studies were

performed on this system because of the fact that the rate could not be increased and that no reactive intermediates could be detected spectroscopically.

Conclusion

Acetyl-uns-penp has not been used in coordination chemistry so far despite its interesting ligand properties and in contrast to related ligands (in which additional pyridine or phenol donor groups are present) that have attracted a lot of interest in amide chemistry recently.[18,27–33,76–78] A copper(II) complex was recently reported, where the carboxamido function of acetyl-uns-penp is no longer truly sp^2 hybridised and the nitrogen atom undergoes a weak interaction with the metal centre.[13] In our present work, we demonstrated that acetyl-uns-penp is capable of influencing coordination chemistry by building hydrogen bonds with hydrogen acceptors in the vicinity of the carboxamido function. The intramolecular hydrogen bond between one arm of the tripodal ligand and a coordinated substrate molecule in **3** suggests a pathway for the second substrate deprotonation step in the reaction cycle of intradiol cleaving catechol dioxygenases according to Scheme 2. Taking into account that the carboxamide can also undergo strong binding interactions with a metal centre upon deprotonation, as demonstrated in **1**, acetyl-uns-penp is a very versatile ligand. Furthermore, structural characterization of two iron(III) complexes of the ligand uns-penp and its catechol dioxygenase reactivity provided additional information on the chemistry of this interesting ligand.

Experimental Section

Materials: All chemicals were obtained from commercial sources and used without further purification.

Caution! *The syntheses and procedures described below involve compounds that contain perchlorate and azide ions, which can detonate explosively and without warning. Although we have not encountered any problems with the compounds used in this study, they should be handled with extreme care.*

Physical Measurements: UV/Vis spectroscopy was performed with a Hewlett–Packard 8453 diode array spectrometer. Elemental analyses were carried out with an Elementar Vario EL III analyzer at the University of Münster.

Syntheses

Ligand Syntheses: The ligand acetyl-uns-penp as well as uns-penp were prepared according to literature procedures.[13]

$[Fe_2$(acetyl-uns-penp)$_2O](ClO_4)_2\cdot H_2O$ (1): Iron(III) perchlorate hexadrate (177 mg, 0.5 mmol) and acetyl-uns-penp (142 mg, 0.5 mmol) were combined in methanol (10 mL). After 10 min of stirring, to the resulting brown solution NaN_3 (49 mg, 0.75 mmol) was added, immediately leading to a very dark red suspension. After 2 h a brown precipitate was filtered off, washed with methanol and diethyl ether, and dried under vacuum. Dark brown prism crystals, air stable and suitable for X-ray diffraction analysis, were obtained by slow evaporation of an acetonitrile solution after 1 week (69 mg, 0.03 mmol, 30%). $C_{16}H_{20}ClFeN_4O_6$ (455.66): calcd. C 42.2, H 4.4, N 12.3; found C 42.6, H 4.2, N 12.7.

1 could also be prepared analogously to the former synthesis except that Et_3N (101 mg, 1.0 mmol) or NaOH (40 mg, 1.0 mmol) were used instead of NaN_3.

[Fe(acetyl-uns-penp)(tcc)Br]$\cdot(C_2H_5)_2O$ (2): Anhydrous iron(III) bromide (30 mg, 0.1 mmol) and acetyl-uns-penp (28 mg, 0.1 mmol) were dissolved in acetone (7 mL). After addition of tetrachlorocatechol hydrate (27 mg, 0.1 mmol) and triethylamine (24 μL, 17 mg, 0.17 mmol) the reaction mixture was stirred for 10 min and filtered. Vapor diffusion of diethyl ether into the complex solution yielded single crystals of **2** (58 mg, 0.09 mmol, 90%), m.p. 181 °C (decomposition). $C_{22}H_{20}BrCl_4FeN_4O_3$ (without solvent, 666.0): calcd. C 39.7, H 3.0, N 8.4; found C 39.0, H 3.9, N 7.9.

[{Fe(acetyl-uns-penp)(tcc)}$_2$O]$\cdot(C_2H_5)_2O\cdot CH_3OH$ (3): The synthetic procedure is identical to the preparation of **2** with the only difference being that a slightly larger amount of triethylamine (28 μL, 20 mg, 0.2 mmol) was used. Vapor diffusion of diethyl ether into the complex solution yielded single crystals of **3** (37 mg, 0.03 mmol, 60%), m.p. 223 °C (decomposition). $C_{44}H_{40}Cl_8Fe_2N_8O_7$ (without solvent, 1188.2): calcd. C 44.5, H 3.4, N 9.4; found C 43.8, H 3.7, N 9.1.

[Fe(uns-penp)Cl$_2$]$\cdot ClO_4\cdot CH_3CN$ (4): To a solution of uns-penp (219 mg, 0.9 mmol) in methanol (10 mL) was added a solution of $Fe(ClO_4)_3\cdot xH_2O$ (139 mg, 0.3 mmol) and $FeCl_3$ (109 mg, 0.6 mmol) in methanol (10 mL). The resulting brown solution was stirred for 1 h at room temperature during which time a greenish yellow solid precipitated, which was then filtered. The precipitate was washed with methanol and diethyl ether, and dried under vacuum. Yellow prism crystals for crystallographic studies were obtained by vapor diffusion of diethyl ether into the acetonitrile solution. Yield: 221 mg (ca. 50%). $C_{16}H_{21}Cl_3FeN_5O_4$ (509.58): calcd. C 37.71, H 4.15, N 13.75; found C 37.59, H 4.13, N 13.68.

[{Fe(uns-penp)Cl}$_2$O]$\cdot(ClO_4)_2\cdot 2CH_3CN$ (5): To a methanol suspension (15 mL) of $Fe(ClO_4)_3\cdot xH_2O$ (115 mg, 0.25 mmol), $FeCl_3$ (41 mg, 0.25 mmol) and uns-penp ligand (122 mg, 0.5 mmol) was added Et_3N (51 mg, 0.5 mmol) in methanol (5 mL) whilst stirring. After 1 h, the resulting greenish brown slurry was filtered and the precipitate was washed with methanol and diethyl ether. Dark brown cubic crystals suitable for X-ray diffraction analysis were obtained by slow evaporation of an acetonitrile solution about 1 week. Yield: 200 mg (ca. 42%). $C_{32}H_{42}Cl_4Fe_2N_{10}O_9$ (964.26): calcd. C 39.86, H 4.39, N 14.53; found C 39.62, H 4.24, N 14.41.

X-ray Crystallographic Studies: Intensity data for **1** were collected with a Siemens SMART CCD 1000 diffractometer using graphite monochromated Mo-K_α radiation (λ = 0.71073 Å) by the ω-scan technique. The collected reflections were corrected for absorption effects.[79] The structure was solved by direct methods and refined by least-squares techniques using the SHELX97 programme package.[80] Further data collection parameters are summarised in Table 2.

Intensity data for acetyl-uns-penp, **2** and **3** were collected with a Bruker AXS SMART 6000 CCD diffractometer (Cu-K_α, λ = 1.54178 Å, Göbel mirror) using the ω-scan technique. The collected reflections were corrected for absorption effects.[79] The structure was solved by direct methods and refined by full-matrix least-squares methods on F^2.[80] Further data collection parameters are summarised in Table 2.

Intensity data for **4** and **5** were collected at a temperature of 100 K with a Bruker-Nonius KappaCCD diffractometer with graphite-monochromated Mo-K_α radiation (λ = 0.71073 Å). Data were corrected for Lorentz and polarization effects. Absorption effects were corrected numerically[81] for **4** and by semi-empirical methods

Table 2. Crystallographic data and experimental details.

Compound	Acetyl-uns-penp	**1**	**2**	**3**	**4**	**5**
Empirical formula	$C_{16}H_{20}N_4O$	$C_{32}H_{40}Cl_2Fe_2N_8O_{12}$	$C_{26}H_{30}BrCl_4FeN_4O_4$	$C_{53}H_{64}Cl_8Fe_2N_8O_{10}$	$C_{16}H_{21}Cl_3FeN_5O_4$	$C_{32}H_{42}Cl_4Fe_2N_{10}O_9$
M_r	284.36	455.66	740.10	1368.42	509.58	964.26
Temperature [K]	140(2)	200(2)	100(2) K	150(2)	100(2)	100(2)
Radiation (λ [Å])	Cu-K_α, 1.54178	Mo-K_α, 0.71073	Cu-K_α, 1.54178	Cu-K_α, 1.54178	Mo-K_α, 0.71073	Mo-K_α, 0.71073
Crystal colour and shape	colourless, cuboid	brown, prism	red, plate	brown, cuboid	yellow, prism	brown, irregular
Crystal size [mm]	0.20 × 0.14 × 0.10	2.00 × 0.40 × 0.50	0.13 × 0.12 × 0.03	0.31 × 0.29 × 0.29	0.24 × 0.15 × 0.12	0.23 × 0.22 × 0.12
Crystal system	triclinic	monoclinic	monoclinic	monoclinic	monoclinic	triclinic
Space group	$P\bar{1}$ (No. 2)	$C2/c$ (No. 15)	$P2_1/c$ (No. 14)	$P2_1/n$ (No. 14)	$P2_1/n$ (No 14)	$P\bar{1}$ (No 2)
a [Å]	9.3758(2)	16.2248(17)	12.4448(5)	10.4477(3)	11.241(1)	8.4308(5)
b [Å]	9.6178(2)	12.8536(13)	13.4022(6)	20.9973(7)	7.8366(6)	11.2769(6)
c [Å]	10.2342(3)	19.653(2)	18.1585(8)	13.9166(5)	24.330(2)	11.8246(8)
α [°]	82.807(2)					71.583(4)
β [°]	68.351(2)	112.910(1)	92.758(3)	94.824(2)	91.443(7)	76.621(5)
γ [°]	62.401(2)					80.422(4)
V [Å^3]	751.10(3)	3775.2(7)	3025.1(2)	3042.1(2)	2142.6(3)	1032.4(2)
Z	2	4	4	2	4	1
$\rho_{calcd.}$ [g·cm^{-3}]	1.257	1.603	1.625	1.494	1.580	1.551
μ [mm^{-1}]	0.652	0.983	9.127	7.570	1.111	1.024
F(000)	304	1880	1500	1412	1044	496
θ range [°]	4.66 to 71.30	2.09 to 28.28	3.56 to 71.35	3.82 to 71.44	3.14 to 27.88	3.30 to 27.87
Index ranges	$-10 \le h \le 11$	$-16 \le h \le 21$	$-14 \le h \le 14$	$-11 \le h \le 12$	$-14 \le h \le 14$	$-11 \le h \le 10$
	$-10 \le k \le 11$	$-17 \le k \le 16$	$-15 \le k \le 16$	$-22 \le k \le 24$	$-10 \le k \le 10$	$-14 \le k \le 14$
	$-11 \le l \le 12$	$-26 \le l \le 26$	$-20 \le l \le 22$	$-15 \le l \le 17$	$-32 \le l \le 32$	$-15 \le l \le 15$
Reflections collected	4369	13663	16266	17174	32406	27493
Unique reflections	2521	4476	5631	5614	5103	4910
R_{int}	0.0285	0.0263	0.0766	0.0650	0.0792	0.0272
Data/restraints/parameters	2521/0/195	4476/0/266	5631/0/368	5614/0/380	5103/0/263	4910/0/260
Goodness-of-fit on F^2	1.099	1.040	0.888	0.954	1.032	1.065
Final R indices [$I > 2\sigma(I)$]	$R1$ = 0.0490	$R1$ = 0.0365	$R1$ = 0.0492	$R1$ = 0.0463	$R1$ = 0.0330	$R1$ = 0.0240
	$wR2$ = 0.1381	$wR2$ = 0.0954	$wR2$ = 0.0981	$wR2$ = 0.1065	$wR2$ = 0.0671	$wR2$ = 0.0580
R indices (all data)	$R1$ = 0.0553	$R1$ = 0.0428	$R1$ = 0.0864	$R1$ = 0.0683	$R1$ = 0.0568	$R1$ = 0.0323
	$wR2$ = 0.1443	$wR2$ = 0.1000	$wR2$ = 0.1082	$wR2$ = 0.1118	$wR2$ = 0.0721	$wR2$ = 0.0606
Largest diff. peak/hole [e·Å^{-3}]	0.210/–0.325	0.937/–0.644	1.458/–0.501	0.400/–0.692	0.401/–0.525	0.434/–0.442

based on multiple scans[79] for **5**. The structures were solved by direct methods; full-matrix least-squares refinement was carried out on F^2 using SHELXTL NT 6.12.[82] All non-hydrogen atoms were refined anisotropically. All hydrogen atoms were geometrically positioned; their isotropic displacement parameters were tied to those of their corresponding carrier atoms by a factor of 1.2 or 1.5.

CCDC-266956 (acetyl-uns-penp), -263645 (for **1**), -266957 (for **2**), -266958 (for **3**), -283894 (for **4**), and -283895 (for **5**) contain the supplementary crystallographic data for this paper. These data can be obtained free of charge from The Cambridge Crystallographic Data Centre via www.ccdc.cam.ac.uk/data_request/cif.

Determination of the Catechol 1,2-Dioxygenase Activity: The catechol cleaving activity of an in situ prepared complex solution was tested using piperidine as an external base as described previously.[61] The amount of base needed to reach the highest reaction rates was determined according to the spectrophotometric titration method described below. To 2 mL of a $2\cdot10^{-4}$ M methanolic solution of $Fe(ClO_4)_3\cdot H_2O$ and the ligand was added a $2\cdot10^{-2}$ M (1 equiv.) solution of 3,5-H_2dbc (0.02 mL). The proper amount of base was added to the reaction mixture from a $2\cdot10^{-2}$ M stock solution. To limit errors, the oxidation of the complex was followed three times by UV/Vis spectroscopy. It is important to note that during these studies iron salts with noncoordinating ions (such as perchlorate or triflate) were used and besides the catecholate ligand no additional coordinating ions (such as bromide used in the crystallographic studies) were present.

Spectrophotometric Titrations: The spectrophotometric titrations were carried out with the same solutions as described above for the activity determinations. To avoid cleavage of the substrate, all manipulations were carried out under argon. A sample of the 3,5-H_2dbc solution (0.1 mL) was added to the complex solution (10 mL). The resulting mixture was titrated with piperidine and the UV/Vis-spectra were monitored using a flow cell (1 cm).

Acknowledgments

We thank the Deutsche Forschungsgemeinschaft (SPP 1118 and SFB 424) and the Fonds der Chemischen Industrie for financial support. M. M. thanks the University of Münster and the International Graduate College "Template Directed Chemical Synthesis" for graduate fellowships.

[1] E. A. Lewis, W. B. Tolman, *Chem. Rev.* **2004**, *104*, 1047–1076.
[2] L. M. Mirica, X. Ottenwaelder, T. D. P. Stack, *Chem. Rev.* **2004**, *104*, 1013–1045.
[3] S. Schindler, *Eur. J. Inorg. Chem.* **2000**, 2311–2326.
[4] M. Costas, M. P. Mehn, M. P. Jensen, L. Que Jr, *Chem. Rev.* **2004**, *104*, 939–986.
[5] S. V. Kryatov, E. V. Rybak-Akimova, S. Schindler, *Chem. Rev.* **2005**, *105*, 2175–2226.
[6] I. Bernal, I. M. Jensen, K. B. Jensen, C. J. McKenzie, H. Toftlund, J.-P. Tuchagues, *J. Chem. Soc., Dalton Trans.* **1995**, 3667–3675.
[7] L. Duelund, R. Hazell, C. J. McKenzie, L. Preuss Nielsen, H. Toftlund, *J. Chem. Soc., Dalton Trans.* **2001**, 152–156.
[8] A. Hazell, C. J. McKenzie, L. P. Nielsen, S. Schindler, M. Weitzer, *J. Chem. Soc., Dalton Trans.* **2002**, 310–317.

[9] A. J. Simaan, F. Banse, P. Mialane, A. Boussac, S. Un, T. Kargar-Grisel, G. Bouchoux, J.-J. Girerd, *Eur. J. Inorg. Chem.* **1999**, 993–996.
[10] A. J. Simaan, S. Dopner, F. Banse, S. Bourcier, G. Bouchoux, A. Boussac, P. Hildebrandt, J.-J. Girerd, *Eur. J. Inorg. Chem.* **2000**, 1627–1633.
[11] J. Kaizer, E. J. Klinker, N. Y. Oh, J.-U. Rohde, W. J. Song, A. Stubna, J. Kim, E. Münck, W. Nam, L. Que Jr, *J. Am. Chem. Soc.* **2004**, *126*, 472–473.
[12] J. Mandel, C. Maricondi, B. Douglas, *Inorg. Chem.* **1988**, *27*, 2990–2996.
[13] M. Schatz, M. Leibold, S. P. Foxon, M. Weitzer, F. W. Heinemann, F. Hampel, O. Walter, S. Schindler, *Dalton Trans.* **2003**, 1480–1487.
[14] G. S. Matouzenko, A. Bousseksou, S. Lecocq, P. J. van Koningsbruggen, M. Perrin, O. Kahn, A. Collet, *Inorg. Chem.* **1997**, *36*, 2975–2981.
[15] C. J. Davies, J. Fawcett, R. Shutt, G. A. Solan, *Dalton Trans.* **2005**, 2630–2640.
[16] J. Mandel, B. Douglas, *Inorg. Chim. Acta* **1989**, *155*, 55–69.
[17] O. Horner, M.-F. Charlot, A. Boussac, S. Un, T. Kargar-Grisel, G. Bouchoux, J.-J. Girerd, *Inorg. Chem.* **1999**, *38*, 1222–1232.
[18] C. Incarvito, M. Lam, B. Rhatigan, A. L. Rheingold, C. J. Quin, A. L. Gavrilova, B. Bosnich, *J. Chem. Soc., Dalton Trans.* **2001**, 3478–3488.
[19] K. Hanaoka, K. Kikuchi, Y. Urano, T. Nagano, *J. Chem. Soc., Perkin Trans. 2* **2001**, *2*, 1840–1843.
[20] H. Sigel, R. B. Martin, *Chem. Rev.* **1982**, *82*, 385–426.
[21] D. S. Marlin, P. K. Mascharak, *Chem. Soc. Rev.* **2000**, *29*, 69–74.
[22] R. J. Guajardo, S. E. Hudson, S. J. Brown, P. K. Mascharak, *J. Am. Chem. Soc.* **1993**, *115*, 7971–7977.
[23] S. Nagashima, M. Nakasako, N. Dohmae, M. Tsujimura, K. Takio, M. Odaka, M. Yohda, N. Kamiya, I. Endo, *Nat. Struct. Biol.* **1998**, *5*, 347–351.
[24] W. Huang, J. Jia, J. Cummings, M. Nelson, G. Schneider, Y. Lindqvist, *Structure* **1997**, *5*, 691–699.
[25] J. C. Noveron, M. M. Olmstead, P. K. Mascharak, *J. Am. Chem. Soc.* **2001**, *123*, 3247–3259.
[26] R. J. Guajardo, F. Chavez, E. T. Farinas, P. K. Mascharak, *J. Am. Chem. Soc.* **1995**, *117*, 3883–3884.
[27] A. K. Patra, R. K. Afshar, M. M. Olmstead, P. K. Mascharak, *Angew. Chem. Int. Ed.* **2002**, *41*, 2512–2515.
[28] D. S. Marlin, M. M. Olmstead, P. K. Mascharak, *Eur. J. Inorg. Chem.* **2002**, 859–865.
[29] A. K. Patra, J. M. Rowland, D. S. Marlin, E. Bill, M. M. Olmstead, P. K. Mascharak, *Inorg. Chem.* **2003**, *42*, 6812–6823.
[30] A. K. Patra, R. K. Afshar, J. M. Rowland, M. M. Olmstead, P. K. Mascharak, *Angew. Chem. Int. Ed.* **2003**, *42*, 4517–4521.
[31] R. K. Afshar, A. K. Patra, M. M. Olmstead, P. K. Mascharak, *Inorg. Chem.* **2004**, *43*, 5736–5743.
[32] J. M. Rowland, M. M. Olmstead, P. K. Mascharak, *Inorg. Chim. Acta* **2002**, *332*, 37–40.
[33] A. K. Patra, P. K. Mascharak, *Inorg. Chem.* **2003**, *42*, 7363–7365.
[34] H. Müller, W. Seidel, H. Görls, *J. Organomet. Chem.* **1994**, *472*, 215–220.
[35] S. V. Kryatov, A. Nazarenko, P. D. Robinson, E. V. Rybak-Akimova, *Chem. Commun.* **2000**, 921–922.
[36] D. M. Kurtz Jr, *Chem. Rev.* **1990**, *90*, 585–606.
[37] T. D. H. Bugg, C. J. Winfield, *Nat. Prod. Rep.* **1998**, *15*, 513–530.
[38] L. Que Jr, R. Y. N. Ho, *Chem. Rev.* **1996**, *96*, 2607–2624.
[39] T. Funabiki, H. Sakamoto, S. Yoshida, L. Tamara, *J. Chem. Soc., Chem. Commun.* **1979**, 754–755.
[40] T. Funabiki, A. Mizoguchi, T. Sugimoto, S. Tada, M. Tsuji, H. Sakamoto, S. Yoshida, *J. Am. Chem. Soc.* **1986**, *108*, 2921–2932.
[41] R. Yamahara, S. Ogo, H. Masuda, Y. Watanabe, *J. Inorg. Biochem.* **2002**, *91*, 151–158.
[42] T. D. H. Bugg, G. Lin, *Chem. Commun.* **2001**, 941–952.
[43] N. Raffard, R. Carina, A. J. Simaan, J. Sainton, E. Riviere, L. Tchertanov, S. Bourcier, G. Bouchoux, M. Delroisse, F. Banse, J.-J. Girerd, *Eur. J. Inorg. Chem.* **2001**, 2249–2254.
[44] W. O. Koch, H.-J. Krüger, *Angew. Chem.* **1995**, *107*, 2928–2931; *Angew. Chem. Int. Ed. Engl.* **1995**, *34*, 2671–2674.
[45] D.-H. Jo, L. Que Jr, *Angew. Chem. Int. Ed.* **2000**, *39*, 4284–4287.
[46] H. G. Jang, D. D. Cox, L. Que Jr, *J. Am. Chem. Soc.* **1991**, *113*, 9200–9204.
[47] M. Pascaly, M. Duda, F. Schweppe, K. Zurlinden, F. K. Müller, B. Krebs, *J. Chem. Soc., Dalton Trans.* **2001**, 828–838.
[48] M. Duda, M. Pascaly, B. Krebs, *Chem. Commun.* **1997**, 835–836.
[49] R. H. Heistand II, R. B. Lauffer, E. Fikrig, L. Que Jr, *J. Am. Chem. Soc.* **1982**, *104*, 2789–2796.
[50] R. H. Heistand II, L. A. Roe, L. Que Jr, *Inorg. Chem.* **1982**, *21*, 676–681.
[51] K. Spartalian, C. J. Carrano, *Inorg. Chem.* **1989**, *28*, 19–24.
[52] P. Mialane, E. Anxolabéhère-Mallart, G. Blondin, A. Nivorojkine, J. Guilhem, L. Tchertanova, M. Cesario, N. Ravi, E. Bominaar, J.-J. Girerd, E. Münck, *Inorg. Chim. Acta* **1997**, *263*, 367–378.
[53] M. Merkel, F. K. Müller, B. Krebs, *Inorg. Chim. Acta* **2002**, *337*, 308–316.
[54] R. Viswanathan, M. Palaniandavar, T. Balasubramanian, T. P. Muthiah, *Inorg. Chem.* **1998**, *37*, 2943–2951.
[55] H. Fujii, Y. Funahashi, *Angew. Chem. Int. Ed.* **2002**, *41*, 3638–3641.
[56] M. Velusamy, M. Palaniandavar, *Inorg. Chem.* **2003**, *42*, 8283–8293.
[57] M. Merkel, M. Pascaly, B. Krebs, J. Astner, S. P. Foxon, S. Schindler, *Inorg. Chem.* **2005**, *44*, 7582–7589.
[58] A. M. Orville, J. D. Lipscomb, D. H. Ohlendorf, *Biochemistry* **1997**, *36*, 10052–10066.
[59] M. W. Vetting, D. A. D'Argenio, L. N. Ornston, D. H. Ohlendorf, *Biochemistry* **2000**, *39*, 7943–7955.
[60] M. I. Davis, A. M. Orville, F. Neese, J. M. Zaleski, J. D. Lipscomb, E. I. Solomon, *J. Am. Chem. Soc.* **2002**, *124*, 602–614.
[61] M. Merkel, D. Schnieders, S. M. Baldeau, B. Krebs, *Eur. J. Inorg. Chem.* **2004**, 783–790.
[62] Y. Dong, H. Fujii, M. P. Hendrich, R. A. Leising, G. Pan, C. R. Randall, E. C. Wilkinson, Y. Zang, L. Que Jr, *J. Am. Chem. Soc.* **1995**, *117*, 2778–2792.
[63] R. M. Buchanan, S. Chen, J. F. Richardson, M. Bressan, L. Forti, A. Morvillo, R. H. Fish, *Inorg. Chem.* **1994**, *33*, 3208–3209.
[64] A. Hazell, K. B. Jensen, C. J. McKenzie, H. Toftlund, *Inorg. Chem.* **1994**, *33*, 3127–3134.
[65] S. Ito, T. Okuno, H. Matsushima, T. Tokii, Y. Nishida, *J. Chem. Soc., Dalton Trans.* **1996**, 4479–4484.
[66] T. Kojima, R. A. Leising, Y. Shiping, L. Que Jr, *J. Am. Chem. Soc.* **1993**, *115*, 11328–11335.
[67] B. R. Whittlesey, Z. Pang, R. A. Holwerda, *Inorg. Chim. Acta* **1999**, *284*, 124–126.
[68] B. Kwak, K. W. Cho, M. Pyo, M. S. Lah, *Inorg. Chim. Acta* **1999**, *290*, 21–27.
[69] E. C. Wilkinson, Y. Dong, L. Que Jr, *J. Am. Chem. Soc.* **1994**, *116*, 8394–8395.
[70] Y. Nishida, T. Okuno, S. Ito, A. Harada, S. Ohba, H. Matsushima, T. Tokii, *Chem. Lett.* **1995**, 885–886.
[71] M. Pascaly, M. Duda, A. Rompel, B. H. Sift, W. Meyer-Klaucke, B. Krebs, *Inorg. Chim. Acta* **1999**, *291*, 289–299.
[72] D. Moon, M. S. Lah, R. E. D. Sesto, J. S. Miller, *Inorg. Chem.* **2002**, *41*, 4708–4714.
[73] S. Yan, D. D. Cox, L. L. Pearce, C. Juarez-Garcia, L. Que Jr, J. H. Zhang, C. J. O'Connor, *Inorg. Chem.* **1989**, *28*, 2507–2509.
[74] R. E. Norman, S. Yan, L. Que Jr, G. Backes, J. Ling, J. Sanders-Loehr, J. H. Zhang, C. J. O'Connor, *J. Am. Chem. Soc.* **1990**, *112*, 1554–1562.

[75] G. Musie, C.-H. Lai, J. H. Reibenspies, L. W. Sumner, M. Y. Darensbourg, *Inorg. Chem.* **1998**, *37*, 4086–4093.
[76] K. Ghosh, A. A. Eroy-Reveles, B. Avila, T. R. Holman, M. M. Olmstead, P. K. Mascharak, *Inorg. Chem.* **2004**, *43*, 2988–2997.
[77] K. Hanaoka, K. Kikuchi, H. Kojima, Y. Urano, T. Nagano, *Angew. Chem. Int. Ed.* **2003**, *42*, 2996–2999.
[78] J. M. Rowland, M. M. Olmstead, P. K. Mascharak, *Inorg. Chem.* **2001**, *40*, 2810–2817.
[79] *SADABS*, Siemens Area Detector Absorption Correction, Siemens.
[80] G. M. Sheldrick, *SHELX-97*, University of Göttingen, **1997**.
[81] P. Coppens in *Crystallographic Computing* (Eds.: F. R. Ahmed, S. R. Hall, C. P. Huber), Munksgard, Copenhagen, **1970**, 255–270.
[82] G. M. Sheldrick, *SHELXTL NT*, Bruker Analytical Instruments, Madison, Version 6.12, **2002**.

Received: October 10, 2005
Published Online: March 1, 2006

